REPORT DOCUMENTATION PAGE

Form Approved OMB No. 0704-0188

1. AGENCY USE ONLY (Leave blank)	2. REPORT DATE	3. REPORT TYPE AND DATES COVERED
	1997	Final Report

4. TITLE AND SUBTITLE

Problem of Supersonic Flow Declaration by Magnetic Field

5. FUNDING NUMBERS

F6170896W0297

6. AUTHOR(S)

Dr. Alexander Vatazhin

7. PERFORMING ORGANIZATION NAME(S) AND ADDRESS(ES)

Central Institute of Aviation Motors
Aviamotornaya St. 2
Moscow 111250
Russia

8. PERFORMING ORGANIZATION REPORT NUMBER

N/A

9. SPONSORING/MONITORING AGENCY NAME(S) AND ADDRESS(ES)

EOARD
PSC 802 BOX 14
FPO 09499-0200

10. SPONSORING/MONITORING AGENCY REPORT NUMBER

SPC 96-4091

11. SUPPLEMENTARY NOTES

12a. DISTRIBUTION/AVAILABILITY STATEMENT

Approved for public release; distribution is unlimited.

12b. DISTRIBUTION CODE

A

13. ABSTRACT (Maximum 200 words)

This report results from a contract tasking Central Institute of Aviation Motors as follows: The contractor will investigate the problem of hypersonic flow control by magnetic field in channels with minimal losses.

14. SUBJECT TERMS

Plasma Physics, Magnetohydrodynamic (MHD), Hypersonic Flow Control

15. NUMBER OF PAGES

32

16. PRICE CODE

N/A

17. SECURITY CLASSIFICATION OF REPORT	18. SECURITY CLASSIFICATION OF THIS PAGE	19. SECURITY CLASSIFICATION OF ABSTRACT	20. LIMITATION OF ABSTRACT
UNCLASSIFIED	UNCLASSIFIED	UNCLASSIFIED	UL

PROBLEM OF SUPERSONIC FLOW DECELERATION BY MAGNETIC FIELD

(The final report on Contract F61708-96-W0297)

A.B.Vatazhin, V.I.Kopchenov, O.V.Gouskov,
V.A.Likhter, E.K.Kholshchevnikova

MOSCOW
1997

CONTENTS

INTRODUCTION

Supersonic flow deceleration by magnetic field and estimation of this process efficiency is the main object of the investigations performed within this contract. In the previous reports [1, 2], supersonic flow deceleration in the axisymmetric duct by the axisymmetric magnetic field generated by solenoid or current loop was studied. The mathematical, physical models and computer code were developed to simulate such flows. Inviscid (Euler equations), viscous laminar and turbulent flows (full Navier-Stokes equations) were analyzed. It was shown that complex interaction of gasdynamic, MHD effects and boundary layer are responsible for the flow structure generation. Moreover, due to this interaction, some unusual effects concerned with MHD interaction parameters S influence on the deceleration process efficiency are observed. The explanation of these effects was presented in [1, 2].

In this report, another scheme of MHD flow control is investigated. This scheme provides the supersonic flow deceleration in the 2-D channel when magnetic field is perpendicular to the flow plane and, depending on wall electric properties, electric energy may be extracted from the duct. This scheme was widely investigated in 1-D approach for MHD generators [3] and, in the case of moderate supersonic Mach numbers, in 2-D formulation [4].

The substantial peculiarity of this report is the analysis of supersonic flow ($M = 5$) deceleration and estimation of irreversible losses in such flows.

The 2-D Euler and 2-D full Navier-Stokes equations are used for the gasdynamic flow description. Two models are used for the electrodynamic field description: the simplified quasi 1-D model [5] and full 2-D model [4].

It is interesting to note that scheme of MHD control considered in this report attracts particular interest because of proposals of its application in the hypersonic propulsion system of aerospace plane [6, 7]. In this connection, the results obtained in this report concerning viscosity influence on the supersonic MHD flow become very important.

All gasdynamic and electric characteristics of this scheme are presented for all considered models.

Additionally two limiting cases are also investigated. One of them is concerned with deceleration process in 2-D duct due to electric energy input to supersonic flow without magnetic field. The second one is the supersonic flow deceleration in the 2-D duct with isolator walls in the end regions of magnetic field.

The resume of the work performed within this contract and some possible directions of future investigations are presented also.

1. TWO-DIMENSIONAL FLOW IN MAGNETIC FIELD NORMAL TO FLOW PLANE

In this report, the hypersonic flow deceleration in 2-D channel by magnetic field that is perpendicular to flow plane is investigated. The channel walls are nonperforated (for fluid) and may be electrodes, sectioned electrodes or isolators (for electric current). The generator regime is considered essentially. But some examples when electric power is not extracted from channel are discussed too.

1.1. Gasdynamic equations. The governing equations for the present analysis are the unsteady compressible 2-D Euler and full Navier-Stokes equations. The time dependency of the governing equations permits the solution to progress from an arbitrary initial guess to the steady state. One can write the full Navier-Stokes equations in 2-D case

$$\frac{\partial \mathbf{U}}{\partial t} + \frac{\partial \mathbf{F}}{\partial x} + \frac{\partial \mathbf{G}}{\partial y} = \mathbf{Q}, \quad \mathbf{F} = \mathbf{F}(\mathbf{U}), \quad \mathbf{G} = \mathbf{G}(\mathbf{U}) \tag{1.1}$$

Here $\mathbf{U}$ is the vector of conservative variables, $\mathbf{F}$ and $\mathbf{G}$ - vectors of fluxes, including viscous stresses

$$\mathbf{U} = \begin{pmatrix} \rho \\ \rho u \\ \rho v \\ \rho e^* \end{pmatrix}, \quad \mathbf{F} = \begin{pmatrix} \rho u \\ \rho u^2 + p - \tau_{xx} \\ \rho uv - \tau_{xy} \\ \rho u h^* - u\tau_{xx} - v\tau_{xy} + q_{hx} \end{pmatrix},$$

$$\mathbf{G} = \begin{pmatrix} \rho v \\ \rho uv - \tau_{yx} \\ \rho v^2 + p - \tau_{yy} \\ \rho v h^* - u\tau_{yx} - v\tau_{yy} + q_{hy} \end{pmatrix}, \quad \mathbf{Q} = \begin{pmatrix} 0 \\ f_x \\ f_y \\ q \end{pmatrix} \tag{1.2}$$

The total enthalpy and energy are defined by

$$h^* = h + \frac{\left(u^2 + v^2\right)}{2}, \quad e^* = e + \frac{\left(u^2 + v^2\right)}{2}, \tag{1.3}$$

where e and h are specific internal energy and enthalpy.

The components of viscous stresses tensor are given by

$$\begin{aligned} \tau_{xx} &= 2\mu \frac{\partial u}{\partial x} - \frac{2}{3}\mu\left(\frac{\partial u}{\partial x} + \frac{\partial v}{\partial y}\right) \\ \tau_{yy} &= 2\mu \frac{\partial v}{\partial y} - \frac{2}{3}\mu\left(\frac{\partial v}{\partial y} + \frac{\partial u}{\partial x}\right) \\ \tau_{xy} &= \tau_{yx} = \mu\left(\frac{\partial u}{\partial y} + \frac{\partial v}{\partial x}\right) \end{aligned} \tag{1.4}$$

Here ρ, p, and $\mathbf{v}$ are density, pressure, and velocity vector, μ is the dynamic viscosity coefficient. This coefficient is supposed to be the function of temperature (Sutherland's viscosity law). The transfer of heat according to Fourier's law of heat conduction may be presented by

$$q_{hx} = -\frac{\mu}{\mathrm{Pr}}\frac{\partial h}{\partial x}, \qquad q_{hy} = -\frac{\mu}{\mathrm{Pr}}\frac{\partial h}{\partial y} \tag{1.5}$$

where Prandtl number $\mathrm{Pr} = \mu c_p/\lambda$ is supposed to be a constant (in laminar case for air Pr=0.72).

The system (1.1) - (1.5) is closed by the relationships for perfect gas with constant heat capacities

$$h = \frac{\gamma}{\gamma - 1}\frac{p}{\rho}, \quad p = \rho \Re T \tag{1.6}$$

Here γ is the specific heat ratio and $\Re$ is gas constant.

In relations (1.2) f_x, f_y and q are correspondingly volume densities of MHD force and electric power supplied to the gas. The expressions for $\mathbf{f}$ and q are following

$$\mathbf{f} = \mathbf{j} \times \mathbf{B}, \quad q = \mathbf{jE} \tag{1.7}$$

Here $\mathbf{B}$, $\mathbf{E}$ and $\mathbf{j}$ are vectors of magnetic field, electric field and electric current density. In (1.7) the volume electric charge density is neglected.

In turbulent case, the averaged full Navier-Stokes equations are used. The Bussinesq hypothesis is used to express the turbulent tenses through tensor of deformation rates defined by averaged velocity components with changing of dynamic viscosity μ on the efficient transport coefficients $\mu_e=\mu+\rho\nu_t$ in equations (1.4). Here ν_t is turbulent viscosity. In equation (1.5), $(\mu/\mathrm{Pr}+\rho\nu_t/\mathrm{Pr}_t)$ are used instead of μ/Pr. Here Pr_t is turbulent Prandtl number.

The one equation differential model "ν_t-91" [8] for turbulent viscosity ν_t is used. This equation can be presented in the following form:

$$\frac{\partial \rho\nu_t}{\partial t} + \frac{\partial \rho u\nu_t}{\partial x} + \frac{\partial \rho v\nu_t}{\partial y} = \frac{\partial}{\partial x}\left[\rho(c_1\nu_t + \nu)\frac{\partial \nu_t}{\partial x}\right] + \frac{\partial}{\partial y}\left[\rho(c_1\nu_t + \nu)\frac{\partial \nu_t}{\partial y}\right] +$$

$$+c_2\rho\nu_t G + c_3\nu_t\left(u\frac{\partial \rho}{\partial x} + v\frac{\partial \rho}{\partial y}\right) - c_4\rho\nu_t^2\frac{G^2}{a^2} - \rho\frac{c_5\nu_t^2 + c_6\nu_t\nu}{S^2}.$$

$$c_2 = c_2'\frac{\nu_t^2 + 11.2\nu_t\nu + 12.8\nu^2}{\nu_t^2 - 11.2\nu_t\nu + 64\nu^2} \tag{1.8}$$

$$G^2 = 2\left(\frac{\partial u}{\partial x}\right)^2 + 2\left(\frac{\partial v}{\partial y}\right)^2 + \left(\frac{\partial u}{\partial y}\right)^2 + \left(\frac{\partial v}{\partial x}\right)^2 + 2\frac{\partial v}{\partial x}\frac{\partial u}{\partial y}$$

c_1	c_2'	c_3	c_4	c_5	c_6
2	0.2	0.7	0.5	3	50

Here a is sound velocity, S is minimal distance to the wall and ν is the kinematic viscosity.

1.2 Two-dimensional electrodynamic model. When induced magnetic field is neglected in comparison with the applied external magnetic field, the equations for **E**, **j** and **B** determination are following [3, 1]

$$\mathbf{j} = \sigma(-\nabla\varphi + \mathbf{v}\times\mathbf{B}) - \alpha(\mathbf{j}\times\mathbf{B}), \quad \text{div}\,\mathbf{j} = 0 \quad (\alpha = \frac{\beta}{|\mathbf{B}|})$$
$$\text{rot}\,\mathbf{B} = 0, \quad \text{div}\,\mathbf{B} = 0, \quad \mathbf{E} = -\nabla\varphi \qquad (1.9)$$

Here φ is electric potential, σ is electric conductivity, β is the Hall parameter, α and σ are known functions of thermodynamic parameters. In these equations **B** is applied magnetic field. The equation $\text{rot}\,\mathbf{B} = 0$ is satisfied in the regions where external electric circuits are absent. It is suggested that transport coefficients (viscosity, conductivity) are not dependent upon the magnetic field **B**.

Let's assume that applied magnetic field has the following structure

$$\mathbf{B} = (B_x(x,z),\ 0,\ B_z(x,z)) \qquad 1.10)$$

Such form of magnetic field is realized in many practical situation when condition $B_x = 0,\ B_z = B_0 = \text{const}$ is fulfilled in the main magnetic field zone and distribution (1.10) is fulfilled in the end zones of magnetic field.

Let's suggest that flow structure and medium properties are following:

$$\mathbf{v} = (u(x,y),\ v(x,y),\ 0), \quad \sigma = \sigma(x,y), \quad \alpha = \alpha(x,y) \qquad (1.11)$$

Procedure of z-averaging of equations (1.9) at above mentioned assumptions was produced in [3]. According [3], the magnetic field is given by

$$\mathbf{B} = (0,\ 0,\ B(x)), \quad B(x) = < B_z(x,z) >_z \qquad (1.12)$$

where $B(x)$ is the known function and $< >_z$ designates the averaging in z - direction.

The solution of (1.9) is sought in the form

$$\mathbf{j} = (j_x(x,y),\ j_y(x,y),\ 0), \quad \varphi = \varphi(x,y) \qquad (1.13)$$

As a result, the following 2-D electrodynamic equations may be formulated:

$$j_x = \sigma_\beta\left[-\frac{\partial\varphi}{\partial x} + vB + \beta\left(\frac{\partial\varphi}{\partial y} + uB\right)\right]$$
$$j_y = \sigma_\beta\left[-\frac{\partial\varphi}{\partial y} - uB + \beta\left(-\frac{\partial\varphi}{\partial x} + vB\right)\right] \qquad (1.14)$$

$$\frac{\partial j_x}{\partial x} + \frac{\partial j_y}{\partial y} = 0 \quad \left(\sigma_\beta = \frac{\sigma}{1+\beta^2},\ \beta = \alpha B\right) \qquad (1.15)$$

From (1.14) - (1.15) the following elliptical equation for φ is obtained

$$\Delta\varphi + \frac{\partial\varphi}{\partial x}\left(\frac{\partial \ln\sigma_\beta}{\partial x} + \beta\frac{\partial \ln(\beta\sigma_\beta)}{\partial y}\right) + \frac{\partial\varphi}{\partial y}\left(\frac{\partial \ln\sigma_\beta}{\partial y} - \beta\frac{\partial \ln(\beta\sigma_\beta)}{\partial x}\right) =$$
$$= \sigma_\beta^{-1}\left\{\frac{\partial}{\partial x}\left[B\sigma_\beta(v + \beta u)\right] - \frac{\partial}{\partial y}\left[B\sigma_\beta(u - \beta v)\right]\right\} \qquad (1.16)$$

The forces f_x, f_y and local electric power q supplied to gas are defined as

$$f_x = j_y B, \quad f_y = -j_x B, \quad q = -j_x\frac{\partial\varphi}{\partial x} - j_y\frac{\partial\varphi}{\partial y} \qquad (1.17)$$

The solution of equation (1.16) requires the formulation of the boundary conditions on the duct walls and in the entry and exit duct cross-sections. The formulation of these boundary conditions depends upon the physical problem.

The following wall boundary conditions will be considered in typical cases of this report.

Walls are ideal electrodes. Then the potential is constant on each wall. Thus

$\varphi = \varphi_- = \text{const}_1$ on the lower wall
$\varphi = \varphi_+ = \text{const}_2$ on the upper wall (1.18)

Walls are ideally sectioned electrodes. In this case the electric potential distributions along the upper and lower walls are supposed to be known. In some cases these distributions may be taken from experiments (see [4]). Thus

$\varphi = \varphi_-(s)$ along the lower wall
$\varphi = \varphi_+(s)$ along the upper wall (1.19)

Here s is coordinate along the wall.

Walls contain electrodes and isolators. Then the electric potentials on the electrodes are constant values. For isolators, the normal component of electric current density on the wall is equal to zero. Thus

$\varphi = \text{const}$ on each electrode
$j_n = 0$ on the isolators (1.20)

It is necessary to note that gasdynamic equations (1.1)-(1.6) along with equation (1.8) for turbulent viscosity can be solved using (1.17). In turn, electrodynamic equations (1.14) -(1.15) can be solved if velocity components are known. Therefore the solution of the whole gasdynamic - electrodynamic problem can be obtained using iterative procedure when the electrodynamic subsystem is solved using known gasdynamic parameters and gasdynamic subsystem is solved taking into account known characteristics of electromagnetic field.

1.3. Quasi one-dimensional electrodynamic model. Simplified electrodynamic models are widely used in technical applications instead of 2-D models. These models are based on the following line of reasoning. When gasdynamic velocities u and v, values of σ and α are dependent only on transverse coordinate y, and magnetic field B, channel height h and electric boundary conditions do not vary with longitudinal coordinate x, the exact solution of equations (1.14)-(1.15) exists. All variables in this solution (may be except for electric potential) are depend only on coordinate y. Let's assume now that $\xi = (u, v, \sigma, \alpha, h, B)$ and boundary conditions vary slightly with x. This assumption allows to use above mentioned solution with $\xi = \xi(x, y)$ as an approximate solution.

This procedure was discussed firstly in [3]. Some examples of such model applications are presented in [5]. The general formulations of main equations for different types of boundary conditions was presented in previous report [2].

In this report, the one version of quasi one-dimensional models will be considered that corresponds to the real situation when electric potential distributions on the upper and on the lower walls are given. In practice, electrodes are sectioned and potential varies along a wall. In numerical modeling, it is convenient to use the wall potential distributions from experiments [4]. The above mentioned quasi one-dimensional approximation for this case is described by equations

$$E_y = \frac{j_y}{\sigma_\beta} + B(u - \beta v) \tag{1.21}$$

$$j_y = -\frac{B\langle u - \beta v\rangle - (\delta\varphi / h)}{\langle \sigma_\beta^{-1} \rangle}, \quad j_x = \sigma v B - \beta j_y \tag{1.22}$$

$$f_x = j_y B, \; f_y = -j_x B, \quad q = j_y E_y, \; (<\xi> = h^{-1}\int_0^h \xi(x,y)dy \;) \tag{1.23}$$

Here $\delta\varphi = \varphi_- - \varphi_+$, h and B are given functions of x. They are the control functions. For f_x, f_y, q we have, according to (1.23), the relationships using only local parameters.

1.4. Dimensionless parameters. The system of equations is used in dimensionless form. The main values used for reference are following: the duct height D_0 at the entry, the free stream velocity V_0, density ρ_0, gas constant $\Re$, dynamic viscosity μ_0, characteristic magnetic field B_*, the reference difference $\delta\varphi_0 = (\varphi_- - \varphi_+)_0$ of electric potential on the duct walls, electric conductivity σ_0 and the value of α_0. Then all coordinates and length are referred to D_0, velocity components to V_0, pressure to $\rho_0 V_0^2$, energy and enthalpy to V_0^2, temperature to $V_0^2/\Re$, viscosity to μ_0 and turbulent viscosity to μ_0/ρ_0, magnetic field intensity to B_*, electric conductivity and α to σ_0 and α_0. Then the following dimensionless parameters appear in the system of equations

$$\mathrm{Re} = \rho_0 V_0 D_0/\mu_0\,,\quad S = \sigma_0 B_*^2 D_0/\rho_0 V_0\,,\quad K_0 = \frac{\delta\varphi_0}{V_0 B_* D_0},\ \mathrm{Pr},\ \mathrm{Pr_t},\ \gamma,\ \beta_0 = \alpha_0 B_*$$

where Re is Reynolds number, S is MHD interaction parameter, K_0 is the load parameter and β_0 is the Hall parameter.

2. THE PROBLEMS FORMULATION

The aim of this work is the investigation of supersonic flow deceleration in channel in the presence of transverse magnetic field for three situations.

1) The supersonic flow deceleration in MHD generator regime. Channel walls, in this case, consist of electrodes, or sectioned electrodes, or electrodes and isolators. Between electrodes on the lower and upper walls, the electric potential difference is induced. The electric power is extracted from a channel.

2) The supersonic flow deceleration as a result of electric power input with no magnetic field. In this case, electric potential difference between electrodes on the lower and upper walls is given. Another part of walls are isolators. The flow deceleration is caused by Joule dissipation into gas.

3) The supersonic flow deceleration in the channel with nonconducting walls as a result of current loops arising in zones with nonuniform magnetic field. Such loops appear ordinarily in the end zones of magnetic field.

In all three cases, the determination of potential distribution in the channel is a main problem.

For main peculiarities detection, the analysis in this report is produced at the assumption that σ and α are constants. Hall parameter is accounted for only in some situations.

In all examples, 2-D duct of constant height is investigated. The duct scheme is presented in Fig. 1. Its entry cross-section is located at coordinate x = - 6 and the exit cross-section at x = 5.5.

Consider outlined problems more widely.

Problem 1. The flow deceleration is provided mainly by magnetic field in the central part of the duct. The magnetic field is applied in lateral direction z in this part of the duct. The magnetic field smoothly abates to the entry and exit cross-sections of the duct. The magnetic field distribution along the duct $B(x)$ is shown in Fig. 1*a. The electric potential difference is induced and supported between upper and lower duct walls in central part of the duct (see Fig. 1*d). The duct is operated in the regime of MHD generator when "electro-motion force" is larger than induced potential difference. The electric potential on each wall approaches to zero in directions to the entry and exit cross-sections of the duct (see Figs. 1*b, c).

The flow at the duct entry is supposed to be supersonic and uniform. All parameters distributions must be given for supersonic flow at the duct entry. In the considered case,

the flow Mach number M_0 at the duct entry is equal to 5. The slip velocity conditions are posed on tube walls in inviscid case and no-slip conditions - in viscous case. For viscous and heat conducting gas the wall temperature is supposed to be equal to free stream temperature in the entry cross-section. The additional boundary conditions are not required on the exit computational boundary in supersonic inviscid flow. In viscous case, the so called drift boundary conditions with normal derivatives of all parameters being determined inside computational region are posed both in supersonic core region and in subsonic part of wall boundary layer.

This problem was solved using both quasi 1-D approach for electromagnetic field (equations (1.21)-(1.23)) and 2-D formulation of the electrodynamic problem (equation (1.16)). In 2-D case, the following boundary conditions are formulated for equation (1.16). The potential distribution along the upper and lover walls is given.

$\varphi = \varphi_-(x)$ along the lower wall and

$\varphi = \varphi_+(x)$ along the upper wall (2.1)

Here x is the coordinate along the wall and $\varphi_-(x)$, $\varphi_+(x)$ approach to zero when x tends to duct entry and exit. The boundary conditions in the entry and exit cross-sections of the duct are following

$$\varphi_i = 0 \quad \text{and} \quad \varphi_e = 0 \tag{2.2}$$

Here indexes "i" and "e" correspond to inlet (entry) and exit cross-sections of the duct.

Two types of electric potential distributions along the wall were considered. In both cases the load parameter K_0 is equal to 0.3. The function $\delta\varphi(x) = \varphi_-(x) - \varphi_+(x)$ is supposed to be fixed in both cases. In the first case, it is supposed that

$$\varphi_+(x) = -\varphi_-(x) = -\delta\varphi(x)/2 \tag{2.3}$$

In the second case the following potential distribution is given along the walls

$$\varphi_+(x) = 0, \quad \varphi_-(x) = \delta\varphi(x) \tag{2.4}$$

The potential distribution along the walls corresponding to relations (2.3) and (2.4) are shown in Figs. 1*b and 1*c.

It is necessary to note that the solution of electrodynamic problem in quasi 1-D approach (1.21)-(1.23) depends only upon the value $\delta\varphi$ (see Fig. 1*d). Therefore the results corresponding to cases (2.3) and (2.4) are identical if this quasi 1-D approach is used.

It is necessary to note that in the case of 2-D electrodynamic problem solution the Hall effects were neglected in this and following problems.

Problem 2. In this case, it is supposed that only electric field is used for flow deceleration. The magnetic field is absent ($B(x)=0$). The upper and lower duct walls are composed of isolator and conductor. The isolator part is located from the entry cross-section $x = -6$ up to $x = -2$ and from the cross-section $x = 3$ up to duct exit at $x = 5.5$. The conductor is located from $x = -2$ up to $x = 3$.

The equation (1.16) for electric potential is transformed to $\Delta\varphi = 0$. The following boundary conditions for φ are posed on the duct walls

$$\varphi_{-}(x) = \delta\varphi / 2 = \text{const}_1, \quad -2 \le x \le 3 \tag{2.5}$$

$$\varphi_{+}(x) = -\delta\varphi / 2 = \text{const}_2, \quad -2 \le x \le 3 \tag{2.6}$$

$\delta\varphi$ is supposed to be equal to the maximal value of $\delta\varphi$ in Problem 1. The normal component of a current density on the isolator wall is set to be equal to zero. Thus the following boundary conditions are fulfilled on the isolator sections of upper and lower walls taking into account condition that $B = 0$

$$\frac{\partial\varphi}{\partial n} = 0, \quad -6 \le x \le -2, \quad 3 \le x \le 5.5 \tag{2.7}$$

The boundary conditions at the inlet and at the exit of the duct are following

$$(j_x)_i = 0, \quad (j_x)_e = 0 \tag{2.8}$$

Problem 3. In this case, only magnetic field is used for flow control. The duct walls are isolated. The magnetic field distribution along the duct is the same as in Problem 1. The duct entry and exit boundary conditions for the electric field are analogues to these ones (2.8) in previous problem. The following boundary conditions are formulated on the isolated duct walls in this case from the condition $\mathbf{j}_n = 0$

$$\frac{\partial\varphi}{\partial y} = -uB \tag{2.9}$$

3. RESULTS

Some calculations in this report were performed on the base of two models. The first model I includes quasi 1-D electrodynamic model (1.21) - (1.23) and 2-D Euler or 2-D Navier-Stokes equations. The second model II includes 2-D electrodynamic model (1.14)-(1.15) or (1.16) and 2-D Euler or 2-D Navier-Stokes equations.

Efficiency of MHD flow deceleration will be characterized in the following way. It is necessary to keep in mind that the gasdynamic variables in the exit cross-section are not uniform when 2-D gasdynamic models are used. In our reports, the averaging procedure (and transition to the equivalent 1-D flow in the exit cross-section) is performed with conservation of mass flow, total enthalpy flux and longitudinal impulse. So, the averaged parameters in the exit section (with index "e") are found. Their ratios to the corresponding parameters in the entry cross-section (index "0") are used as characteristics of the deceleration process.

In addition, it is necessary to consider some parameters that characterize an efficiency of MHD generator. In accordance with [3, 1], the coefficients η and η_N are introduced. The coefficient η is defined as the ratio of power extracted from the duct to the work of the gas against the magnetic field drag:

$$\eta = N/A,$$

where $N = -\iint\limits_D \mathbf{j}\mathbf{E}dxdy$, $A = -\iint\limits_D \mathbf{V}\mathbf{f}dxdy$, D is the flow region and $\mathbf{f}$ is electromagnetic force.

The coefficient η_N is defined as the ratio of power extracted from the duct to the flow of total enthalpy at the duct entry

$$\eta_N = N / \int\limits_F \rho u h^* dy,$$

where integral is calculated over the duct entry cross-section.

3.1. One example of model testing. In report [1], the one-dimensional MHD flow in crossed magnetic and electric fields was considered. It was suggested that B=const, E=const, σ = const, β = 0, all gasdynamic variables depend only on x and generator regime is realized. Now, this situation (with the same magnetic and electric fields) was analyzed on the base of 2-D Euler equations. All inlet parameters in this 2-D case were assumed to be uniform. Calculations on the base of 2-D Euler code coincided completely with one-dimensional results. All parameters in the outlet cross-section are the same as in Table 1 of report [1].

3.2. Results for model I (2-D flow and quasi 1-D electrodynamics). The main calculations are performed for the 2-D duct of constant height. The geometry of the duct is presented in Fig. 1. The perfect gas with adiabatic constant $\gamma = 1.4$ is considered. The electric conductivity σ is assumed to be a constant value. If Hall effect is considered, the value α in relation (1.15) is chosen to be constant also. The MHD interaction parameter S in performed calculations is equal to 0.1. The maximal difference of electric potentials between lower and upper walls is chosen as value $\delta\varphi_0$. The load parameter K_0 estimated by the value $\delta\varphi_0$ is equal to 0.3. The magnetic field distribution is shown in Fig. 1*a. Potential difference between lower and upper walls $\delta\varphi$ is shown in Fig.1*d. The entrance Mach number $M_0 = 5$.

The calculation results are presented in Table. The exit to entry pressures p_e/p_0 and total pressures p_e^* / p_0^* ratios, Mach number in the exit cross-section M_e, temperatures ratio T_e / T_0 are used for the estimation of deceleration efficiency. Coefficients η and η_N are introduced for efficiency estimations of electric energy generation. Cases 1-11 correspond directly to the problem examined in given paragraph. The Hall effect were accounted for in cases 2, 7, 11.

The solution of 2-D Euler equations was obtained in cases 1 and 2. The Hall effect was ignored in the case 1. The case 2 was considered to estimate the influence of the Hall effect. In this case the parameter β_0 is equal to 1. The Mach number fields are shown in Figs. 1 and 3 correspondingly for cases 1 and 2. It is obvious that with the use of quasi 1-D electrodynamic approach, the flow which is uniform at the duct entry remains uniform (in normal direction) through all the duct. This fact is illustrated by Fig. 1. In the case 2, the asymmetry of the flow due to Hall effect is generated (see Fig. 2). It is necessary to note that efficiency of deceleration is decreased (the pressure and temperature ratios are diminished, and exit Mach number is increased) when Hall effects are considered. Moreover, the Hall effect provides the diminishing of efficiency of electric energy production characterized by coefficients η_N. This conclusion is consistent with known general theoretical result [3] for ideal electrodes. The modest decrease of the coefficient η for $\beta_0 = 1$ in the solution obtained within 2-D gasdynamic equations and quasi 1-D electrodynamics, which includes the 2-D effects through the averaged values in (1.21) - (1.23), can be indeed explained by the influence of nonuniformity of parameters distribution in 2-D case.

The cases 3-7 correspond to viscous laminar flow with the Reynolds number 5000. The Mach number field for the case 3 without magnetic and electric fields is shown in Fig. 3. Only a fair deceleration of the flow due to viscosity forces is observed in this case. When magnetic field and potential difference $\delta\varphi$ are applied, the developed separation regions are induced in the duct. The calculations for the cases 4-6 are performed when Hall effect is neglected.

The distinctive peculiarity of obtained separation flow pictures in the symmetric duct is the asymmetric flow field structure. Some cases (4-6) were analyzed. In all cases the data obtained for the case 3 (Fig. 3) without electromagnetic fields were chosen as the initial data for the time relaxation process when electromagnetic field is switching on. In the case 4 (Fig. 4), the lower wall was supposed to be thermally adiabatic during a short time interval after electromagnetic field switching on. The Mach number field for this case is shown in Fig. 4. In this case the asymmetric flow field is realized with large separation region on the lower wall. Only small separation region is realized on the upper wall of the duct.

In the case 5 (Fig. 5), the fully symmetric boundary conditions were fulfilled at the duct walls after electromagnetic field switching on, during all time relaxation process. It is interesting to note that the flow field is visually symmetric to some instants of time during the time relaxation process. However, the picture becomes asymmetrical when large separation region is formed in the duct. It is necessary to note that the flow picture in the case with symmetrical boundary conditions during time relaxation process contains large separation region on the upper wall and small separation region on the lower wall. The flow picture for this case is illustrated in Fig. 5. If to compare data presented in Table (cases 4 and 5) corresponding to use of nonsymmetric (during short time only) thermal boundary conditions and to use of fully symmetric boundary conditions (for all relaxation process) then it is obvious that these two cases are fully identical. Moreover, the flow fields are also identical if to identify the upper wall in the case 4 with the lower wall in the case 5 and vice versa.

The case 6 was calculated for the comparison with cases 4 and 5 when only one half of duct was considered. In this case the symmetry condition on the duct symmetry plane is formulated. The flow picture for this case is shown in Fig. 6. It is interesting to note that the deceleration of the flow in asymmetric case (case 5) is slightly more strong with somewhat higher total pressure losses.

Of course, it seems to be questionable that in symmetrical duct at symmetrical boundary conditions on the duct walls and at the uniform flow at the duct entry the flow field in the duct is asymmetric. The convergence to the steady state solution is reached in

both these cases (Figs. 5 and 6). The residual in the case of asymmetric steady state solution and symmetric one when calculation starts from the identical symmetrical initial flow fields (steady solution without electromagnetic field) falls to identical values in these two cases.

The reasons of calculations convergence to the asymmetric steady state solution may be following. Firstly, as was shown earlier, the short in time, asymmetry in boundary conditions may produce the final asymmetric steady state solution. Further, in the case of fully symmetrical boundary conditions the small asymmetry data are presented due to some asymmetrical details in the method of the numerical solution of equations system. This asymmetry is concerned with the pattern for the choosing of minimal derivatives when higher order accuracy monotone scheme is realized. Moreover, the direct and inverse sweeping in the solution of algebraic system of finite difference equation for implicit scheme also introduces some asymmetry. Therefore, it is desirable to perform some methodical work to investigate the possible influence of asymmetrical features of the method on the final steady state solution.

In general case, it may be assumed that symmetrical solution with large separation regions on the duct walls (Fig. 6) is unstable to small asymmetrical disturbances.

Estimating the plausibility of the obtained asymmetrical solutions, it is necessary to point out on some experimental data [9]. These data were obtained at the duct throttling. It was detected that in real ducts sometimes asymmetrical shock train system is observed. True, some unsteady effects are observed at the duct throttling as a rule. Therefore it is necessary to provide some additional investigations to confirm the existence of asymmetrical solutions at symmetrical wall boundary conditions due to instability of symmetrical solutions to small asymmetrical disturbances.

The case 7 was considered to analyze the influence of the Hall effect both on the flow fields and on the efficiency of deceleration and electric power generation processes. The influence of the Hall effects on the flow field can be estimated if to compare Figs. 5 and 7. It is possible to see that Hall effects in this situation provides the more symmetrical flow field than in case when Hall effect is ignored.

This, at the first sight, unusual result is explained as follows. The solution for isotropic conductivity is asymmetric (see Fig. 5). The large separation region was initiated by boundary layer separation due to force f_x acting in upstream direction. In the presence of Hall effect, the force f_x decreases and separation region dimensions are reduced. On the

other hand, appearing force f_y acts in the $(-y)$-direction, to the lower wall, and pressure increase near the lower wall is responsible for separation zone arising.

As it usually is, in the presence of Hall effect, the flow deceleration is less intensive and extracted electric power is less than for case $\beta_0 = 0$.

To analyze the turbulent regimes, the cases 8 - 11 were considered. In this case the entry part of the duct was elongated two times in comparison with shown in Figs. 1-7 to provide the generation of appreciable boundary layer at the entry to operational part of the channel. The flow fields analyzed are shown in Figs. 8 - 11 when the boundary layer is given at the duct entry cross-section and parameters are fixed in this cross-section. The Reynolds number in this case is equal to 10^6. In cases 9 and 10 Hall effect is ignored. The development of the flow in the duct at given entry conditions without electromagnetic field (case 8) is illustrated by Fig. 8. The data presented in Table confirm that some deceleration takes place in the duct due to the boundary layer. When electromagnetic field is switched on, the separation region is realized in the duct. The asymmetrical flow picture is realized in this case. The developed separation region arises on the upper wall and unseparated flow is observed on the lower duct wall. This flow picture is qualitatively similar to this one obtained in laminar case (compare with Fig. 5). The difference is that in laminar case the small separation region is generated also on lower wall in contrast to turbulent case.

The results presented in Fig. 9 (case 9) and in Fig. 10 (case 10) are obtained at the identical conditions. The only difference is that the solution for case 10 was obtained within "symmetrical" formulation of the problem when only half of the duct was considered with symmetry conditions on the symmetry plane of the duct. It is necessary to note that in case 9 the deceleration of asymmetrical flow is less intensive in comparison to symmetrical flow.

The influence of the Hall effect ($\beta_0 = 1$) on the turbulent flow in the duct is investigated in case 11 (Fig. 11). The comparison with data presented in Fig. 9 ($\beta_0 = 0$) demonstrates that the Hall effect, as in laminar flow, diminishes the asymmetry in the flow. The boundary layer and separation region thickness on the upper wall is reduced considerably in the zone of MHD flow control. The Hall effect influence on the intensity of deceleration is minor. It is possible to note the reduction of η in the case with Hall effect.

Thus, the following conclusion can be made on the base of this 2-D flow calculations with quasi 1-D electrodynamics model (model I). The results calculated within this approach show the dramatic influence of 2-D effects on the flow field in viscous case in comparison with results obtained within widely used 1-D inviscid approach. It is necessary to

note that 2-D Euler equations solutions practically coincide with results of 1-D inviscid flow calculations if Hall effects are neglected. Moreover, the data show that the deceleration intensity is substantially less in 2-D viscous case than in 1-D inviscid estimations. The electric energy generated in the channel diminishes also considerably if 2-D effects are taken into account in comparison with 1-D inviscid case. The influence of Hall effect on the deceleration process is less prominent in 2D viscous flow in comparison with 1-D inviscid flow. The influence of the Hall parameter on the electric energy extracted from the duct is also more noticeable in 1-D inviscid case.

3.3. Results for model II (2-D flow and 2-D electrodynamics). Some calculations were performed for the Problem 1 in inviscid case for 2-D flow using 2-D electrodynamic model when Hall parameter $\beta = 0$. The gasdynamic parameters at the duct entry are the same as in the previous paragraph in the case of quasi 1-D electrodynamics. The boundary conditions for the electrodynamic problem (1.16) on the duct walls are chosen in accordance with (2.1). The following variants were considered. The case 12 corresponds to the wall electric potential distribution in accordance with (2.3), and case 13 - in accordance with (2.4). In these two cases the inlet and entry boundary conditions for electrodynamic problems are formulated in accordance with (2.2). The magnetic field distribution was chosen as in the previous section (Fig. 1*a). Therefore it is possible to compare results obtained in cases 12 and 13 with those for case 1. It is interesting to note that the solutions within the quasi 1-D model are equivalent for conditions corresponding to the cases 12 and 13.

The following data are presented for each of these two cases: the lines of equal electric potential (Figs.12a and 13a), the "streamlines" of electric current (current lines in Figs. 12b and 13b) and Mach number fields (Figs. 12c and 13c). Figures 12 and 13 correspond to the cases 12 and 13. Notice that the electric potential lines in these two cases are different due to boundary conditions on the wall. The current lines in Figs. 12b and 13b are practically normal to the duct walls in the central part of the duct and current is directed from the upper wall to the lower one. The well expressed end effects are observed at the entry and exit from the region where magnetic field is applied. The end effects in current lines manifest by different manner in these two cases. The Mach number fields are shown in Figs. 12c and 13c. The presence of 2-D effects as in electric field as in flow fields is obvious from these figures. Some asymmetry relatively to plane of symmetry in Mach number field is observed for the case 13 which is caused by asymmetry of electric field. Comparison with data obtained in the case 1 (with quasi 1-D electrodynamycs) shows that influence of 2-D electrodynamic effects on the deceleration efficiency is negligible. This fact is confirmed by the data presented in Table.

The viscous laminar flow at the Reynolds number 5000 with symmetric distribution of $\delta\varphi$ (see (2.3) and Fig.1*b) was calculated in the case 14. The electric potential, current and Mach number fields are shown in Fig. 14. In this case, the asymmetrical separated flow similar to this one in Fig. 4 is realized. The deceleration intensity in this case diminishes in comparison with cases 12 and 13. The electric energy generated in the duct is also reduced in this case in comparison to inviscid case if to compare the values of coefficient η_N. The comparison of obtained results for this case with those for case 5 shows that the difference in the flow fields and in deceleration characteristics is not appreciable. Some difference is observed only in coefficients η and η_N. It is interesting to note that in viscous case the deceleration is not so intensive as in inviscid case. This is caused by extensive separation regions with small velocities, where the MHD interaction is weak.

Thus, it is possible to conclude that in considered special examples the 2-D flow calculations with quasi 1-D electrodynamic equations (model I) provide acceptable accuracy for the estimation of integral characteristics of deceleration process. However, some details especially the end MHD effects can not be resolved exactly using quasi 1-D approach. Moreover, the possibility of end effects to cause the essential difference in aforementioned integral performances in more complex flows must not be ruled out.

3.4. Results for supersonic flow deceleration due to electric power input without magnetic field. The following case 15 is concerned with the Problem 2 for inviscid flow when magnetic field is absent and applied electric potential difference between lower and upper walls $\delta\varphi_0$ is the same as in previous case. The duct walls are composed of isolator and conductor sections. The boundary conditions for electrodynamic problem are formulated in accordance with (2.5) - (2.8). Electric potential field, current lines and Mach number field are shown in Figs. 15a - 15c. It is interesting to point out the terminal effects which take place in the vicinity of the cross-sections where isolated and conducting walls are joint. The current picture (like "roll") is similar to this one in the case when 2-D electric field is defined in the duct with the rest medium (without magnetic field; see, for example, [3]). It is necessary to note that in contrast to previous cases the electric current flows from lower wall to upper one. The electromagnetic force $\mathbf{f} = 0$ in this case due to absence of magnetic field. However the supersonic flow is heated and decelerated due to electric power supply to the flow. At given electric field parameters, this deceleration is sufficiently weak. But the influence of this effect on the supersonic flow deceleration will be enhanced if the potential difference will be increased.

3.5. Results for supersonic flow deceleration in the end zones of magnetic field. The final Problem 3 is solved for inviscid flow when the duct walls are isolated and the applied magnetic field has left and right end zones. The boundary conditions (2.8) for electrodynamic problem are formulated at the duct entry and exit. The boundary conditions (2.9) are fulfilled at the isolated duct walls. The electric potential contours for this case 16 are shown in Fig. 16a. At the entry to region where the magnetic field is applied and at the exit from this region two closed recirculation current regions are generated (see Fig. 16b). The direction of rotation is clockwise in region at the entry to magnetic field and counter-clockwise in the exit region. The existence of such current recirculation regions, at given MHD interaction parameter $S = 0.1$, causes the appreciable irreversible losses in the flow at very weak flow deceleration. The irreversible losses and flow deceleration will be strongly enhanced if MHD interaction parameter S will be of the order 1.

TABLE

Case number	p_e/p_0	p_e^*/p_0^*	M_e	T_e/T_0	η	η_N
1	4.69	0.0575	1.879	3.10	0.358	0.116
2	2.94	0.112	2.61	2.36	0.335	0.0715
3	1.57	0.351	3.81	1.44	-	-
4	2.35	0.148	2.93	1.91	0.504	0.0539
5	2.35	0.148	2.93	1.91	0.504	0.0539
6	2.29	0.156	2.99	1.88	0.516	0.0561
7	2.27	0.163	3.02	1.88	0.433	0.0434
8	1.26	0.577	4.36	1.21	-	-
9	2.84	0.114	2.64	2.26	0.474	0.0622
10	3.61	0.0784	2.25	2.63	0.411	0.0856
11	2.88	0.113	2.62	2.28	0.369	0.0618
12	4.74	0.0571	1.87	3.14	0.349	0.113
13	4.85	0.0563	1.84	3.19	0.329	0.106
14	2.34	0.150	2.95	1.91	0.462	0.048
15	1.73	0.360	3.76	1.69	-	-
16	1.21	0.664	4.50	1.19	-	-

CONCLUSION

The problem of supersonic flow deceleration of conducting gas in 2-D channel of constant height by lateral magnetic field that is normal to the plane of gasdynamic flow in the MHD generator regime is considered. The electric field is analyzed using simplified quasi 1-D electrodynamic model or full 2-D formulation.

It is shown on the test examples that 2-D and especially viscous effects are very important at the estimations of efficiency of supersonic flow deceleration by magnetic field. The deceleration intensity and electric power generation efficiency are not so promising as those obtained from traditional simplest models.

The decrease of deceleration intensity in viscous case in comparison with inviscid one and especially with 1-D case is caused by the origin of large separation regions in the duct at the deceleration. The recirculation regions of small velocities are really switched off from the MHD influence on the flow.

These factors should be taken into account in the investigations of possibilities to use MHD effects, of the type considered in this report, in hypersonic propulsion system. Therefore the estimations concerning the efficiency of MHD control of hypersonic propulsion system obtained in 1-D approach or even in 2-D approach, but without viscosity effect, must be revised taking into account 2-D and viscous effects necessarily.

For the viscous MHD flow in the duct with large separation regions, two different steady state solutions were obtained: symmetrical and asymmetrical. It is possible to suppose the instability of the symmetrical flow with large separation region in the duct to small asymmetrical disturbances in the duct. Some additional methodical investigations are necessary for this phenomena justification and explanation.

RESUME

of the main results obtained within three stages of work on the contract

1. The following classical problems on the supersonic flow deceleration by magnetic field in the duct were solved in this work using 1-D approach, 2-D Euler and 2-D full Navier - Stokes equations:

a) the supersonic flow deceleration in the circular tube by axisymmetric magnetic field;

b) the supersonic flow deceleration in 2-D duct by the magnetic field which is perpendicular to the plane of flow in the MHD generator regime;

c) the supersonic flow deceleration in 2-D duct at the electric energy supply to the flow without magnetic field;

d) the supersonic flow deceleration in the end regions of magnetic field in a 2-D duct with isolated walls.

2. The results of the work allow to conclude that estimations obtained with the aid of usual 1-D approach must be revised. It is shown that MHD influence on the flow due to special distribution of force and heat sources dramatically changes the flow structure in comparison with this one obtained within 1-D approach. The recirculation zones, cavities, boundary layer separation regions with separation points located upstream of the MHD interaction zone, shock systems are generated in the flow. The reasonable estimations of irreversible and total pressure losses in the duct can be obtained only on the base of calculations accounting for these space effects.

3. The calculation of the scramjet elements flow with the magnetic field must be performed taking into account viscosity effects within the full Navier - Stokes equations for laminar and turbulent regimes. The modern turbulence models must be used in the last case. The calculations which were performed in this work show that the viscosity gives rise to unexpected, at first glance, effects. For example, some regimes exist at high Reynolds numbers for flow in circular tube when the MHD interaction parameter S increase is followed by decrease of flow deceleration (instead of deceleration enhancement) in usual situation. The comparison of results obtained in calculations of viscous and inviscid flows shows that, in some situations, the flow deceleration intensity may decrease in viscous case instead of usual increase of supersonic flow deceleration due to viscous effects.

4. Some preliminary experience is gained due to this work in the choosing of magnetic field distribution which provides the control of specific flow features: separation re-

gion length, reattachment of separation region in the given point on the wall, velocity profile.

5. The gained experience, developed physical and gasdynamic models, computer codes and obtained results allow to formulate problems concerned with using of MHD control in hypersonic propulsion system.

THE POSSIBLE FUTURE WORK DEVELOPMENT

On the base of existing and our new models and computer codes, it is possible to consider some problems concerning the control of hypersonic flow by the magnetic field in the scramjet duct. The MHD control may be carried out using different electrical regimes (power extraction or input).

The following problems can be solved.

1. *MHD control of flow deceleration in the hypersonic inlet.* The MHD influence on the inlet shock system to provide the design conditions when shocks must be focused on the inlet leading edge cowl for different points of flight trajectory. The MHD action on the flow in the internal part of the inlet duct to provide the better conditions for compression by control both the velocity profiles and separation region. Use of combined gasdynamic and MHD effects on the hypersonic flow to provide the best hypersonic inlet performances. Comparison of the performances of inlets of usual gasdynamic, MHD and combined (gasdynamic and MHD) schemes.

2. The integration of hypersonic propulsion system with a vehicle gives rise to thick boundary layer at the engine entrance. Therefore it is interesting to consider the following problem: the boundary layer MHD control on the forebody of a hypersonic vehicle to provide the better conditions for the inlet and propulsion system operation.

3. The investigation of possibility to improve the performances of hypersonic propulsion system by MHD redistribution of energy in the engine duct. It is known that at high flight Mach numbers the temperature at the supersonic combustor entry is too high to provide the efficient fuel combustion. The large part of energy contained in fuel is used unefficiently due to large losses on the dissociation. The large part of energy is consumed on the generation of radicals in the chemical reactions. These intermediate products of chemical process are not recombined in the engine duct up to the engine exit. These effects essentially reduce the total efficiency of hypersonic propulsion system. It seems to be promising to provide the hypersonic flow deceleration using MHD influence in generator regime at the engine entrance. Possibly, this provision can provide the better conditions for combustion of the fuel. Then the extracted energy is supplied to the duct flow in MHD accelerator regime at the exit from the combustor or in the nozzle. The system of codes developed in CIAM for scramjet flow analysis along with new developed physical models for MHD control allows to provide such investigation and to estimate the total propulsion system efficiency.

4. The essential source of scramjet efficiency losses is assosiated with the development of the thick boundary layer in the engine duct. In accordance with aforementioned infor-

mation, the thick boundary layer at the engine entry is caused by integration effects of propulsion system and vehicle forebody. This thick boundary layer interacts with shock system in the propulsion system duct. As the result of this interaction the boundary layer separation in the scramjet duct arises especially taking into account the thermal throttling. Therefore it is interesting to investigate the possibility of velocity profile control in the duct by the magnetic field using the well known **Hartman effect** (when velocity profile becomes more uniform). Three model problems can be solved on the first stage. One of them is the development of supersonic viscous laminar and turbulent flow in the duct with magnetic field perpendicular to the walls. The second problem is concerned with shock-boundary layer interaction in the presence of magnetic field. The third problem is the MHD control of the flow in the duct when thermal throttling takes place due to the chemical reactions.

REFERENCES

1. *A.B.Vatazhin, V.I.Kopchenov, O.V.Gouskov, V.A.Likhter, E.K.Kholshchevnikova.* Problem of supersonic flow deceleration by magnetic field (The first stage report on Contract F61708-96-W0297), Moscow, 1997.

2. *A.B.Vatazhin, V.I.Kopchenov, O.V.Gouskov, V.A.Likhter, E.K.Kholshchevnikova.* Problem of supersonic flow deceleration by magnetic field (The second stage report on Contract F61708-96-W0297), Moscow, 1997.

3. *Vatazhin A.B., Ljubimov G.A., Regirer S.A.* Magnetohydrodynamic flows in channels. Moscow, Nauka. 1970. 672 p. [In Russian]

4. *Borghi C.A., Cristofolini A., Ribani P.L.* A time-dependent two-dimensional analysis of transients in plasma MHD generators. 12th International Conference of magnetohydrodynamic electric power generation. Yokohama, Japan, Oct. 15 - 18, 1996, V. 2, p. 807.

5. *Ivanov V.A.* A method for calculation a MHD flow with boundary layer separation. High Temperature. 1994. V. 32, N 6, pp. 909-912.

6. *Gurijanov E.P., Harsha P.T.* AJAX: New Directions in Hypersonic Technology. AIAA Paper, 96-4609.

7. *Bityurin V.A., Zeigarnik V.A.* On Perspective of MHD Technology in Aerospace Applications. AIAA Paper, 96-2355.

8. *Gulyaev A.N., Kozlov V.Ye., Secundov A.N.* A universal one-equation model for turbulent viscosity. Fluid Dynamics, v. 28, N. 4, 1993, pp. 485-494.

9. *Ikui T., Matsuo K., Nagai M.* The Mechanism of Pseudo-Shock Waves. Bulletin of the JSME. Vol. 17. June 1974. pp. 731-739.

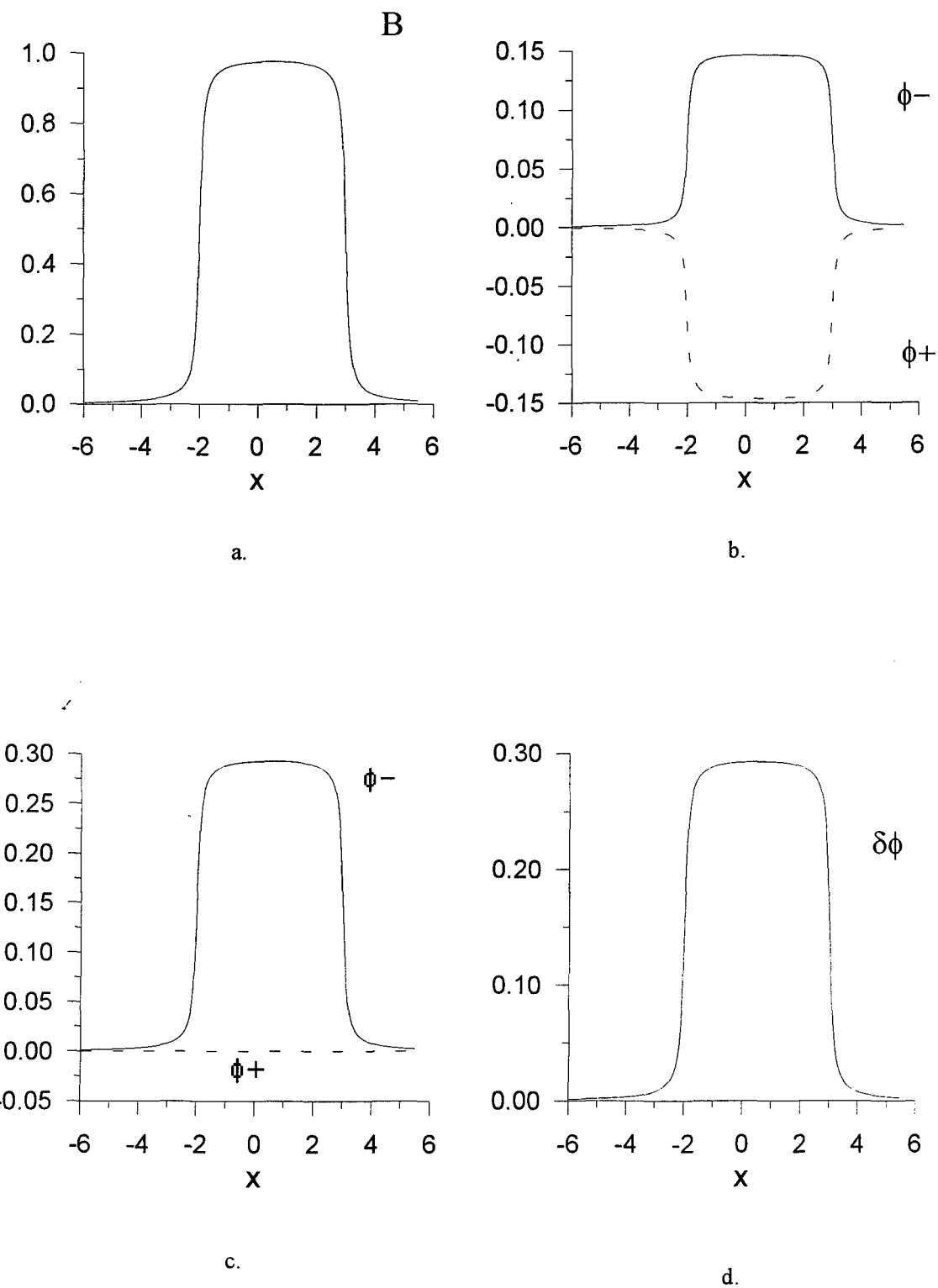

Fig.1*. Distribution of magnetic field (a), electric potentials φ^- and φ^+ along lower and upper walls (variants b and c), electric potentials difference between walls (d)

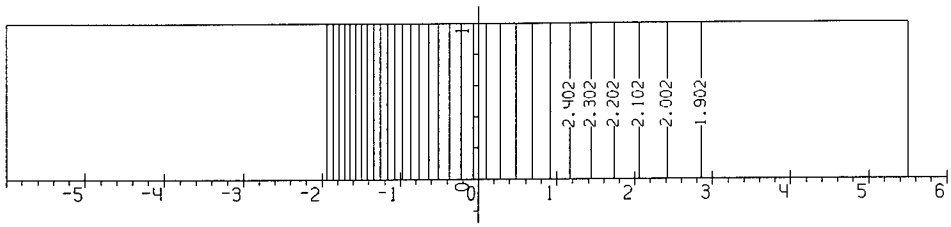

Fig.1. Mach number field
Case 1. M_0=5, S=0.1, K_0=0.3, β_0=0
inviscid flow, quasi 1-D electrodynamics
B(x) distribution as in Fig.1*a, $\delta\varphi(x)$ distribution as in Fig. 1*d

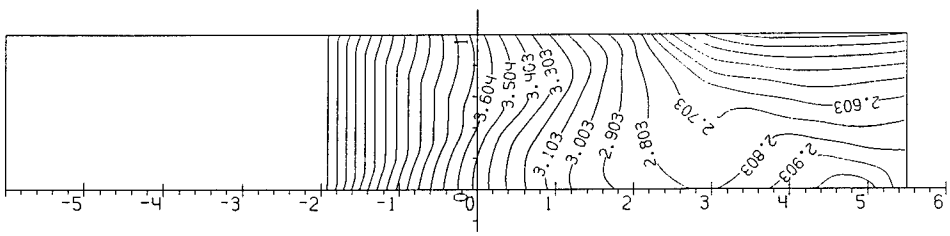

Fig.2. Mach number field
Case 2. M_0=5, S=0.1, K_0=0.3, β_0=1
inviscid flow, quasi 1-D electrodynamics
B(x) distribution as in Fig.1*a, $\delta\varphi(x)$ distribution as in Fig. 1*d

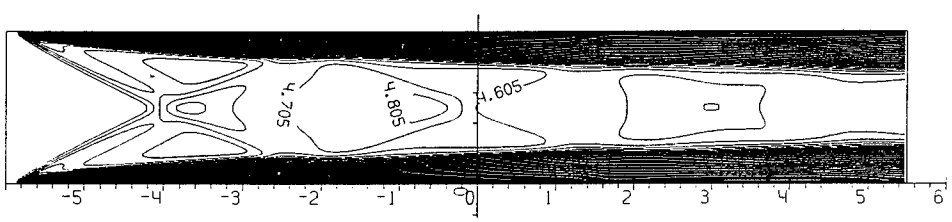

Fig.3. Mach number field
Case 3. M_0=5, S=0.1, K_0=0.3, β_0=0
viscous laminar flow, $Re=5\times10^3$
magnetic and electric fields are absent

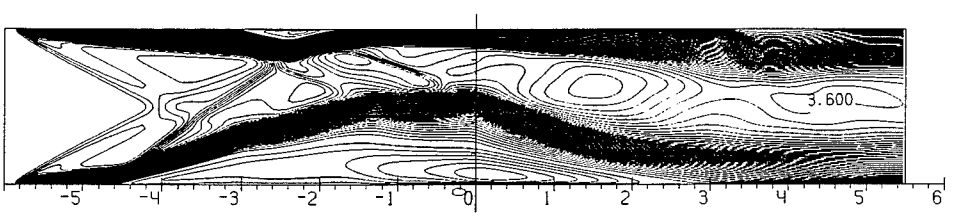

Fig.4. Mach number field
Case 4. M_0=5, S=0.1, K_0=0.3, β_0=0
viscous laminar flow, $Re=5\times10^3$, quasi 1-D electrodynamics
B(x) distribution as in Fig.1*a, $\delta\varphi(x)$ distribution as in Fig. 1*d

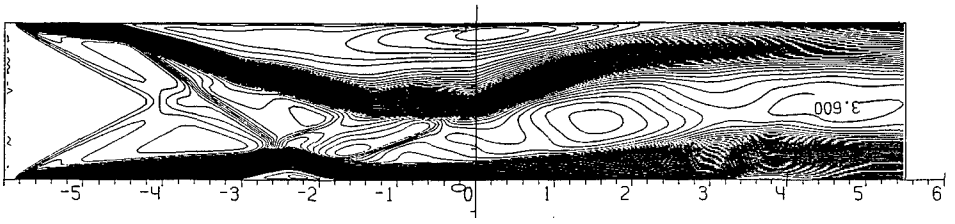

Fig.5. Mach number field
Case 5. $M_0=5$, $S=0.1$, $K_0=0.3$, $\beta_0=0$
viscous laminar flow, $Re=5\times10^3$, quasi 1-D electrodynamics
B(x) distribution as in Fig.1*a, $\delta\varphi(x)$ distribution as in Fig. 1*d

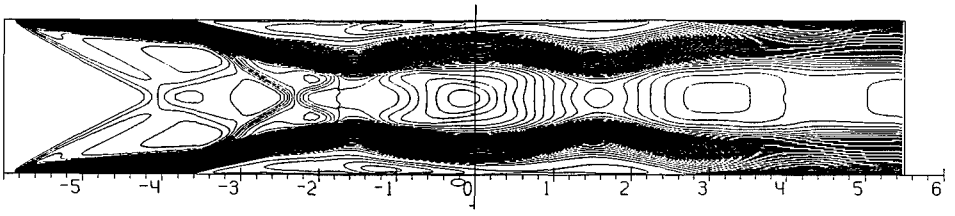

Fig.6. Mach number field
Case 6. $M_0=5$, $S=0.1$, $K_0=0.3$, $\beta_0=0$
viscous laminar flow, $Re=5\times10^3$, quasi 1-D electrodynamics
B(x) distribution as in Fig.1*a, $\delta\varphi(x)$ distribution as in Fig. 1*d
symmetrical formulation

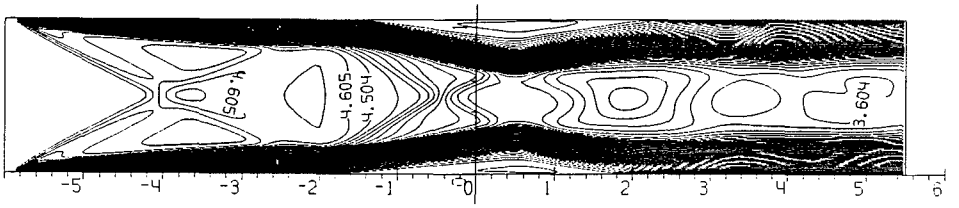

Fig.7. Mach number field
Case 7. $M_0=5$, $S=0.1$, $K_0=0.3$, $\beta_0=1$
viscous laminar flow, $Re=5\times10^3$, quasi 1-D electrodynamics
B(x) distribution as in Fig.1*a, $\delta\varphi(x)$ distribution as in Fig. 1*d

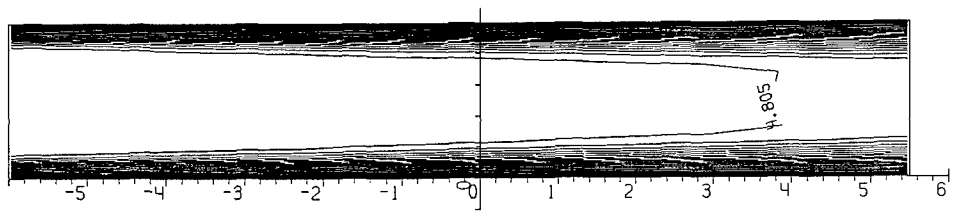

Fig.8. Mach number field
Case 8. M_0=5, S=0.1, K_0=0.3, β_0=0
turbulent flow, Re=10^6
magnetic and electric fields are absent

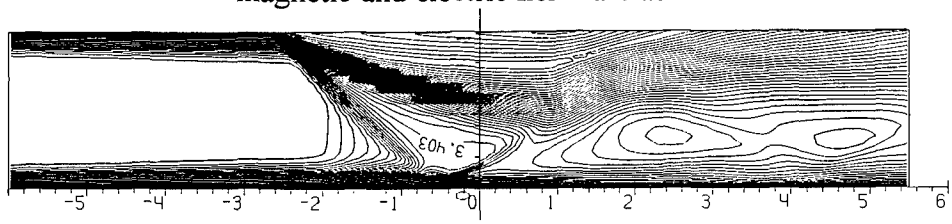

Fig.9. Mach number field
Case 9. M_0=5, S=0.1, K_0=0.3, β_0=0
turbulent flow, Re=10^6, quasi 1-D electrodynamics
B(x) distribution as in Fig.1*a, $\delta\varphi$(x) distribution as in Fig. 1*d

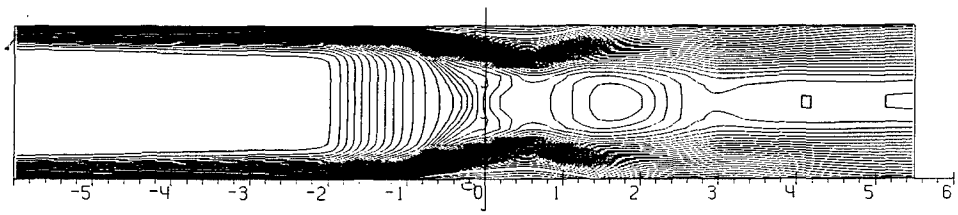

Fig.10. Case 10. Mach number field
Case 10. M_0=5, S=0.1, K_0=0.3, β_0=0
turbulent flow, Re=10^6, quasi 1-D electrodynamics
B(x) distribution as in Fig.1*a, $\delta\varphi$(x) distribution as in Fig. 1*d
symmetrical formulation

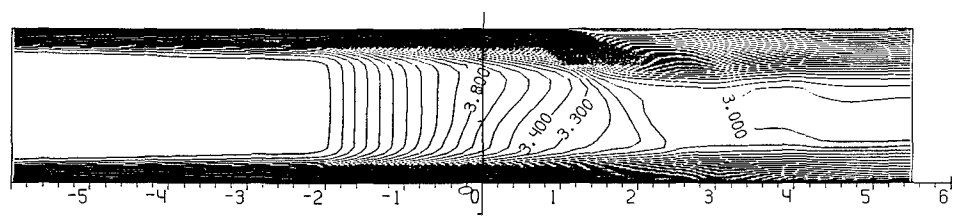

Fig.11. Case 11. Mach number field
Case 11. M_0=5, S=0.1, K_0=0.3, β_0=1
turbulent flow, Re=10^6, quasi 1-D electrodynamics
B(x) distribution as in Fig.1*a, $\delta\varphi$(x) distribution as in Fig. 1*d

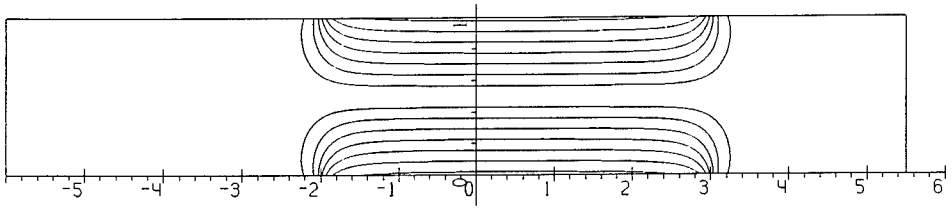

a. Equipotential lines

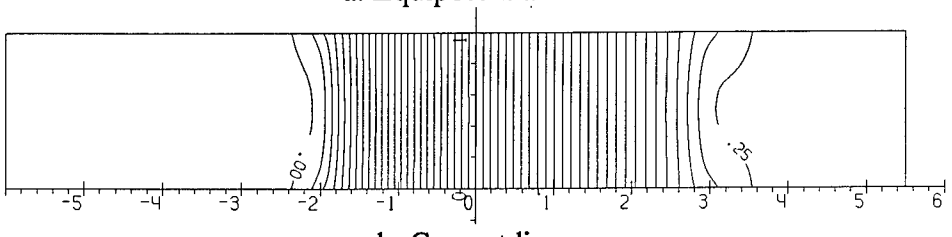

b. Current lines

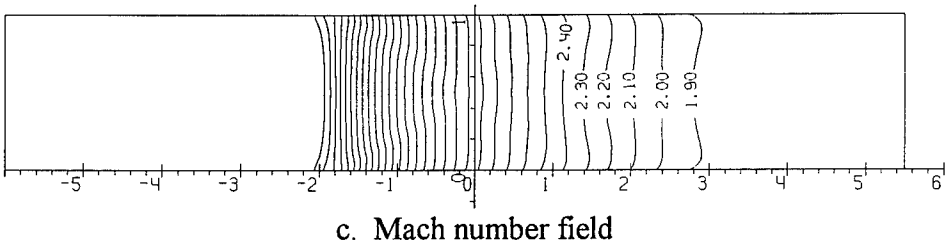

c. Mach number field

Fig.12. Case 12. M_0=5, S=0.1, K_0=0.3, β_0=0
inviscid flow, 2-D electrodynamics
B(x) distribution as in Fig.1*a, $\varphi^+(x)$ and $\varphi^-(x)$ distribution as in Fig. 1*b

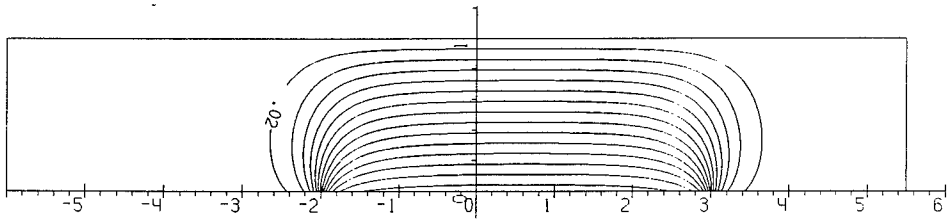

a. Equipotential lines

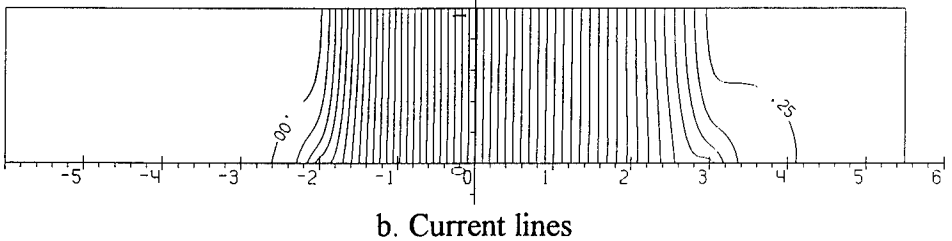

b. Current lines

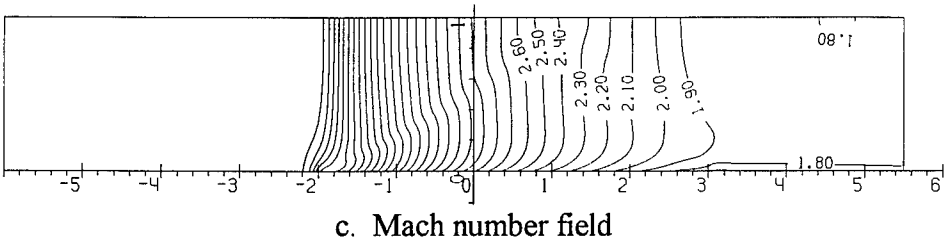

c. Mach number field

Fig.13. Case 13. M_0=5, S=0.1, K_0=0.3, β_0=0
inviscid flow, 2-D electrodynamics
B(x) distribution as in Fig.1*a, $\varphi^+(x)$ and $\varphi^-(x)$ distribution as in Fig. 1*c

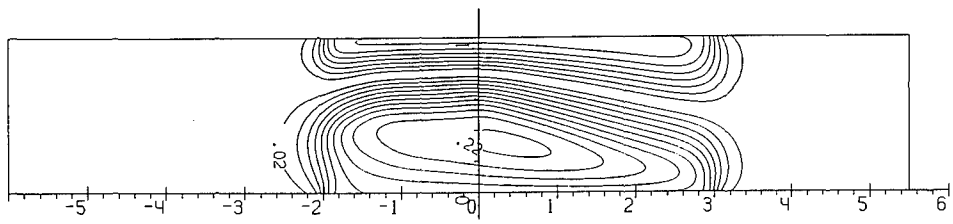

a. Equipotential lines

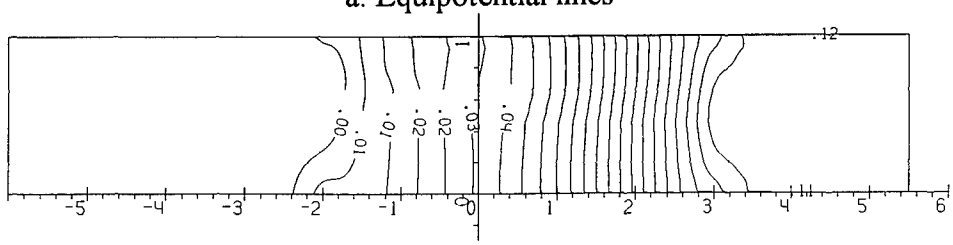

b. Current lines

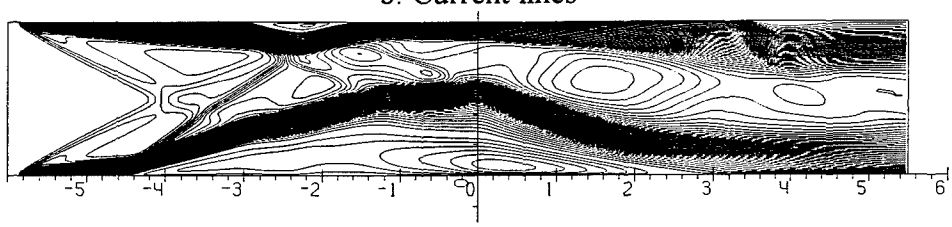

c. Mach number field

Fig.14. Case 14. M_0=5, S=0.1, K_0=0.3, β_0=0
viscous laminar flow, Re=5×10^3, 2-D electrodynamics
B(x) distribution as in Fig.1*a, $\varphi^+(x)$ and $\varphi^-(x)$ distribution as in Fig. 1*b

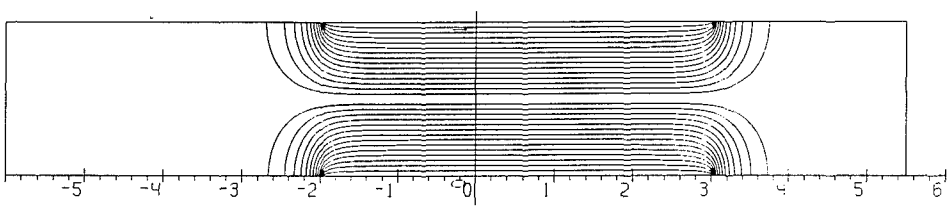

a. Equipotential lines

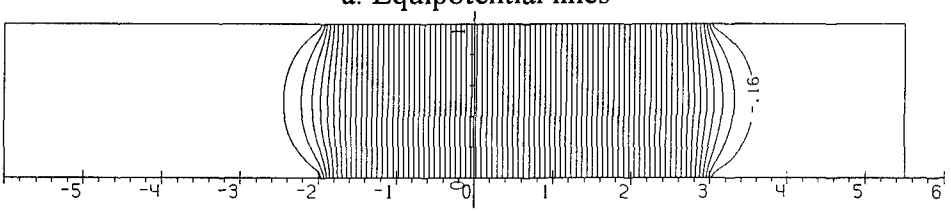

b. Current lines

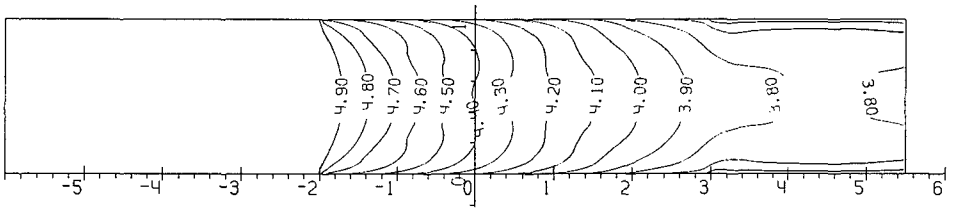

c. Mach number field

Fig.15. Case 15. M_0=5, S=0.1, K_0=0.3, β_0=0
inviscid flow, 2-D electrodynamics
wall sections -2<x<3 - electrodes, other sections - isolators
magnetic field is absent

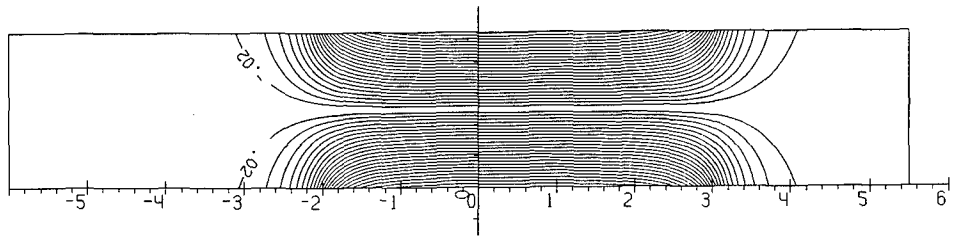

a. Equipotential lines

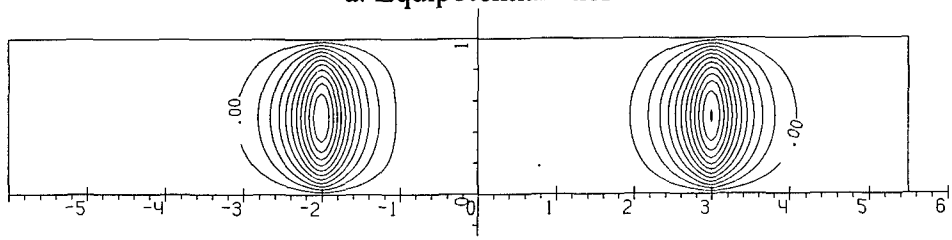

b. Current lines

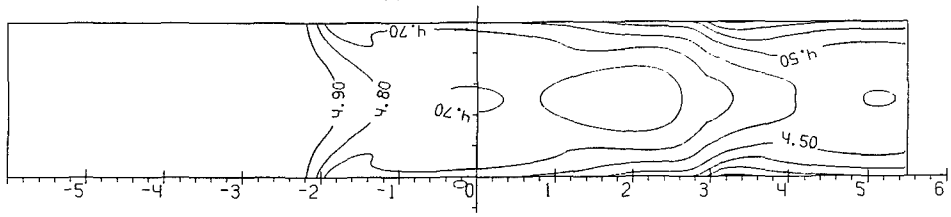

c. Mach number field

Fig.16. Case 16. M_0=5, S=0.1, K_0=0.3, β_0=0
inviscid flow, 2-D electrodynamics
walls are isolators, B(x) distribution as in Fig.1*a